Flexibility in noisy cell-to-cell information dynamics

Ismail Qunbar,[1,*] Michael Vennettilli,[2,*] and Amir Erez[1,†]
[1]*Racah Institute of Physics, The Hebrew University of Jerusalem, Jerusalem 9190401, Israel*
[2]*AMOLF, Science Park 104, 1098 XG Amsterdam, The Netherlands*

(Received 10 July 2024; accepted 10 November 2024; published 10 December 2024)

The exchange of molecules allows cells to exchange information. How robust is the information to changes in cell parameters? We use a mapping between the stochastic dynamics of two cells sharing a stimulatory molecule and parameters akin to an extension of Landau's equilibrium phase transition theory. We show that different single-cell dynamics lead to the same dynamical response—a flexibility that cells can use. The companion equilibrium Landau model behaves similarly, thereby describing the dynamics of information in a broad class of models with coupled order parameters.

DOI: 10.1103/PhysRevResearch.6.043252

I. INTRODUCTION

In the choreography of life, cells respond to environmental stimuli by detecting chemical signals and secreting molecules. This process, fundamental to cellular communication, has attracted much attention, and recent advances in our understanding of information transfer in biological systems include quantifying the energy cost of information transmission in coupled receptors [1], interpreting positional information and spatial coupling [2,3], establishing bounds on the energy cost of transmitting information in various settings [4], and outlining essential trade-offs between cost and predictive power [5]. These studies underscore the complexity and efficiency of cellular communication using molecular exchange and highlight the importance of understanding how cells manage and optimize information exchange. However, despite the dynamic nature of cellular environments, a scaling theory for cell-to-cell information dynamics under changing conditions has yet to be developed.

Our previous work described a minimal model of feedback in cellular sense-and-secrete dynamics [6] and investigated how pairs of such cells share information [7]. For example, upon antigen stimulation, T cells exhibit a bimodal distribution of doubly phosphorylated extracellular signal-regulated kinase (ERK) (ppERK), a critical protein that initiates cell proliferation and determines the immune response [8–10]. We were able to show that a broad class of models, including Schlögl's second model, can be used to explain and extract key features from single-cell measurements of ppERK [6,11]. Here, we extend this line of inquiry to explore how time-varying individual cellular properties impact overall information exchange. How does information in a minimal sense-and-secrete two-cell system respond to gradually changing cellular parameters? We demonstrate that inherent flexibility allows one cell to match the dynamics of the other, in a choreographed dance, so that in a broad class of models, cell-to-cell information is maintained, and key observables scale universally.

Our minimal model of cellular sense-and-secrete dynamics maps a class of well-mixed stochastic biochemical feedback models, in steady state, to parameters analogous to those in Landau's thermal equilibrium phase transition theory. Although applicable to other stochastic models, we focused specifically on mapping the dynamics of Schlögl's second model [12,13] as if it were a Landau theory. Instead of stochastic reaction rates, one may describe the dynamics with an effective reduced temperature θ, magnetic field h, and a magnetizationlike order parameter m [6,7]. These parameters can be extracted from biological data without fitting or knowledge of the underlying molecular details [6]. The stochastic dynamics are never in thermal equilibrium, and the noise is demographic in nature. For this reason we will refer to the Schlögl model at steady state and the Landau model at thermal equilibrium as "companion" systems. The critical transition from a finite to a zero "magnetization" in the Landau theory is equivalent to the bifurcation point of the stochastic dynamics [14]—between a bimodal state, having both high and low molecule counts as stable points the dynamics fluctuate about—to a unimodal state with an intermediate molecule count (see Appendix A). Near the transition point, the correlation time of the system diverges, exhibiting critical slowing down, as expected from the Landau theory [11].

A diverging timescale and critical slowing down do not matter much when considering systems at equilibrium or steady state. In contrast, in a dynamically changing setting, collective properties are expected to be influenced by the slowing down of the collective dynamics. The two-cell system (cells X and Y) has four main parameters: two "fields" (h_X, h_Y) that control overall molecule count bias in each cell and two "reduced temperatures" (θ_X, θ_Y) that act as a bifurcation parameter. The steady state can be described by two collective coordinates: H and T. These collective coordinates dictate both the steady-state mutual information between the

*These authors contributed equally to this work.
†Contact author: amir.erez1@mail.huji.ac.il

cells and the autocorrelation time of the molecule count, which are closely related [7,15]. In this two-cell collective state, each individual cell's reaction rates can be set away from its critical point, while the two-cell collective system remains at criticality. Because the collective state is critical, both the mutual information and the correlation time are maximized; to gain information at steady state one must "pay" with an increased correlation time [7]. Importantly, the collective coordinates H and T are steady-state, linearized solutions that need not apply to the system's dynamics. Here, we consider the universal properties of the two-cell response to time-varying conditions.

Can the system's dynamical changes be described using the collective coordinates, disregarding each cell's specific dynamics? In this paper, we demonstrate that they can be. Therefore, diverse single-cell parameter trajectories can lead to identical systemic responses, allowing substantial flexibility in single-cell properties without impacting the two-cell information. This flexibility in single-cell behavior enhances robustness and evolutionary adaptability, facilitating the exploration of advantageous strategies. Furthermore, while our focus is on cell-to-cell communication, manifested through the stochastic nonequilibrium dynamics of the Schlögl model, our study of the companion Landau model reveals a similar degeneracy in the analogous equilibrium system. This extension of equilibrium Landau theory has been used in the context of phase transitions in minerals and surface and hydration forces [16–18]. Therefore, this study describes a general class of models with coupled order parameters, both equilibrium and nonequilibrium, that bifurcate according to the Ising mean-field universality class.

This paper is a direct continuation of our previous work [7], in which we developed the theory under steady-state conditions. In contrast, the current study focuses on dynamical changes and presents a rigorous dynamical scaling analysis. Our main contribution is demonstrating that numerous different single-cell trajectories can lead to the same two-cell behavior. The rest of this paper is organized as follows: After a brief recap of the model, we compare the steady state of the stochastic dynamics of the extended Schlögl model to its equilibrium Landau companion. We then dynamically ramp both cells' parameters across the bifurcation or critical point, showing the lag in the dynamical response of the ramped system and its scaling. Finally, we show how different single-cell trajectories, sharing the same collective coordinates, lead to identical responses in the information exchange between the two cells.

II. MODEL AND MAPPING TO LANDAU'S EQUILIBRIUM PHASE TRANSITION THEORY

Within each cell, biochemical reactions in a complex signaling cascade result in the net production and degradation of a molecular species of interest. As illustrated in Fig. 1(a), in the first (second) cell, species X (Y) can be produced spontaneously from bath species at rate k_1^+ (q_1^+) and can be produced nonlinearly at rate k_2^+ (q_2^+) via a trimolecular reaction involving two existing X (Y) species and a bath species. Species X (Y) can be degraded linearly with molecule number at a rate k_1^- (q_1^-) or, in a reaction involving three existing X (Y)

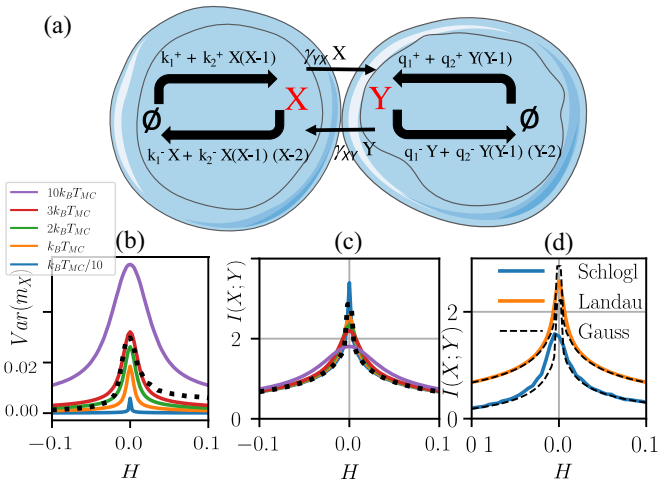

FIG. 1. Schematic of the two-cell model and its steady state. (a) Representation of the two-cell version of the stochastic dynamics, which extend Schlögl's second model [12] similarly to our previous paper [7]. (b) Varying the Monte Carlo temperature $k_BT_{\rm MC}$ in the Landau model affects some observables, e.g., the variance of m_X. The Schlögl model (black dots) exhibits a dependence on H which cannot be captured by tuning the Landau model's $k_BT_{\rm MC}$, reflecting its nonequilibrium nature. (c) The mutual information in the Landau model depends only weakly on $k_BT_{\rm MC}$ and closely matches the Gaussian analytic result (black dots), although at $T = H = 0$ the mutual information in the Gaussian case diverges. (d) Comparison of the mutual information of the two-cell system as a function of the collective field H. Blue line: the nonequilibrium Schlögl steady state; orange line: the extended Landau model at thermodynamic equilibrium; Dashed black line: the analytic results from the Gaussian approximation. Here, both cells are identical: $h_x = h_y = h$ and $\theta_x = \theta_y = 0$, with $n_c = 1000$.

molecules, at rate k_2^- (q_2^-). In addition to the internal reactions, X (Y) can be exchanged from the neighboring cell at rate γ_{xy} (γ_{yx}). Mechanistically, this can be through a gap junction or through diffusion [7].

Reiterating our previous work [6,11], we use a mapping from Schlögl to Landau-like parameters. Without exchange ($\gamma = 0$), the deterministic dynamics corresponding to the reactions in the left cell in Fig. 1(a) are $dX/dt = k_1^+ - k_1^- X + k_2^+ X^2 - k_2^- X^3$, where we have neglected the small shifts of -1 and -2 for large X. These shifts account for the fact that once a molecule decreases in number by 1, the reaction probability changes, but at a large molecule number this change is insignificant. Defining the order parameter $m = (X - n_c)/n_c$, this magnetization is the scaled deviation from the typical molecule number n_c. We choose n_c to eliminate the term quadratic in m, leading to the Landau form [6],

$$\frac{dm}{d\tau} = h - \theta m - \frac{m^3}{3}, \tag{1}$$

where we have defined $n_c = k_2^+/3k_2^-$, $\tau = (k_2^+)^2 t/3k_2^-$, $\theta = 3k_1^- k_2^-/(k_2^+)^2 - 1$, and $h = 9k_1^+(k_2^-)^2/(k_2^+)^3 - 3k_1^- k_2^-/(k_2^+)^2 + 2/3$. The number of molecules in the system is controlled by n_c, which controls all scaling properties of the single-cell system, acting as a *finite system size* of the equivalent critical Ising system [6,11]. The system size

is determined by the ratio of the nonlinear production and degradation terms; intuitively, increasing the production increases the system size.

In steady state, $dm/d\tau = 0$. We can thus interpret m as an order parameter for the single-cell system, $\theta \equiv (T - T_c)/T_c$ as a reduced temperature, and h as a dimensionless field. Analogous to the Ising model, when $h = 0$ in the single-cell system and the reduced temperature, which acts as a bifurcation parameter, $\theta > 0$, the system is in a unimodal steady-state distribution. For $\theta < 0$, the steady state is a bimodal distribution. Similarly, positive or negative h biases the distribution to higher or lower molecule count, respectively. In terms of the Schlögl rates, the nonlinear production rate k_2^+ controls all timescales together with the system size since $\tau = n_c\, k_2^+ t$. For the system to be in its bimodal state, $k_B T/k_B T_c < 1$, so $\theta + 1 < 1$, and thus, $k_1^- < n_c\, k_2^+$. Therefore, bimodality requires that the spontaneous degradation rate k_1^- be smaller than the nonlinear production rate k_2^+ times the system size n_c. Similarly, for $\theta = 0$, satisfying $h > 0$ means that $k_1^+ > \frac{1}{3} n_c^2\, k_2^+$, so to deviate up from the typical molecule count, k_1^+ needs to be larger than the scaled nonlinear production rate.

Applying the same mapping to two coupled cells (with $k \to q$ for Y) results in the Landau form,

$$\frac{dm_X}{d\tau} = h_X - \theta_X m_X - \frac{m_X^3}{3} + g_{XY} m_Y - g_{YX} m_X,$$
$$\frac{dm_Y}{d\tau} = h_Y - \theta_Y m_Y - \frac{m_Y^3}{3} + g_{YX} m_X - g_{XY} m_Y. \qquad (2)$$

In this context, $g_{XY} = 3\gamma_{xy} k_2^- /(k_2^+)^2$ and $g_{YX} = 3\gamma_{yx} q_2^- /(q_2^+)^2$ represent intercellular exchange terms. For simplicity, we set $g_{XY} = g_{YX} = g = 1$ throughout this paper.

Although Eq. (2) is a reparameterization of the nonequilibrium stochastic dynamics of the extended Schlögl model [Fig. 1(a)], one may separately consider it to be an extension of the well-known Landau model [Eq. (1)], computed at thermal equilibrium. This extension of equilibrium Landau theory to two bilinearly coupled order parameters has been considered before in the context of phase transitions in minerals [16], surface and hydration forces [17], and more generally [18]. Here, we focus on the biological system, with its nonequilibrium stochastic dynamics, while in parallel demonstrating similar dynamical scaling results for the companion Landau theory computed at thermal equilibrium.

Linearizing the deterministic steady state ($\frac{d}{d\tau} = 0$) of the Landau form [Eq. (2)] gives the collective coordinates

$$T = \theta_X \theta_Y + g(\theta_X + \theta_Y),$$
$$H = g(h_X + h_Y) + (h_X \theta_Y + h_Y \theta_X)/2. \qquad (3)$$

These collective coordinates, H and T, act as an effective field and effective temperature for the stochastic two-cell system described in the Landau parameters. They account for the collective system's bias towards a higher or lower number of molecules (positive and negative H, respectively) and as a bifurcation parameter between a unimodal ("centralized") and bimodal ("polarized") molecule count distribution (positive and negative T, respectively) [7]. The effect of H when $T = 0$ is shown in Fig. 2; although $T = 0$ in this paper, for completeness, the effect of T is shown in Appendix A in Fig. 5. At the critical point, $T = H = 0$, the two cells exhibit critical slowing down and maximal mutual information between X and Y, regardless of each cell's individual h and θ values.

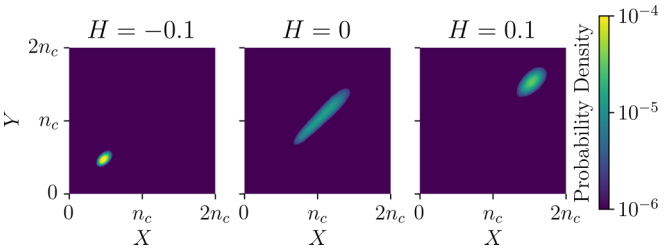

FIG. 2. The effect of H at steady state in the two-cell model. The heat maps show the joint probability distribution $P(X, Y)$, calculated from Gillespie simulations of the two-cell Schlögl model. The color map corresponds to $\ln_{10} P$. Note that for $H = 0.1$, the increased number of molecules results in a wider distribution when compared to $H = -0.1$, whereas the width of the distribution at $H = 0$ is due to the critical behavior. In all simulations, $h_X = h_Y$, and $\theta_X = \theta_Y = 0$ (therefore, $T = 0$), with $n_c = 1000$.

For convenience, Table I is an annotation glossary for the variables used in this paper.

III. RESULTS

A. Mutual information at steady state

We simulated the Schlögl system's stochastic dynamics using the Gillespie algorithm [19,20] and the equilibrium fluctuations of the companion Landau model with the Metropolis-Hastings Monte Carlo algorithm. The dynamics in the Landau case are taken as "model A" in the Halperin-Hohenberg classification [21,22],

$$\frac{dm_X}{d\tau} = -\Gamma \frac{\delta L}{\delta m_X} + \zeta(\tau), \qquad (4)$$

with a similar expression for m_Y, with Γ setting the relaxation timescale of the system and $L = -h_X m_X + \frac{1}{2}\theta_X m_X^2 + \frac{1}{12} m_X^4 - h_Y m_Y + \frac{1}{2}\theta_Y m_Y^2 + \frac{1}{12} m_Y^4 + \frac{1}{2}\, g\, (m_X - m_Y)^2$. The noise $\zeta(t)$ is Gaussian white noise obeying $\langle \zeta \rangle = 0$ and $\langle \zeta(\tau)\zeta(\tau') \rangle = \delta(\tau - \tau')D$. In the equilibrium statistical mechanics sense, to calculate the partition function or, alternatively, to compute expectation values of observables using the Monte Carlo simulation accept/reject, we require a simulation temperature, which we refer to as $k_B T_{\rm MC}$. The long-time limit of the dynamics as a Fokker-Planck equation approaches the equilibrium solution with $P(m_X, m_Y) \propto \exp(-\frac{2\Gamma L}{D})$ and, accordingly, a fluctuation-dissipation relation, $D = 2\Gamma k_B T_{\rm MC}$ [22]. To set the equilibrium temperature $k_B T_{\rm MC}$ we resort to a heuristic argument: Near the bifurcation point of the dynamics, $(\theta = 0, h = 0)$, we have mean$[X] \sim$ Var$[X] \sim n_c$, and therefore, Var$[m_X] =$ Var$[X]/n_c^2 \sim 1/n_c$. Away from $H = 0$ but at $|H| \ll g$, the Gaussian approximation gives Var$[m_X] \sim k_B T_{\rm MC}$ [see Appendix B, Eq. (B9)]. Therefore, $k_B T_c \sim 1/n_c$. However, tuning the precise value of $k_B T_{\rm MC}$ in comparison to the stochastic simulations of the Schlögl model is pointless since the steady state of the Schlögl model does not comply with the equilibrium form, $\exp(-\frac{2\Gamma L}{D})$. Therefore, the probability distribution of m_X and an observable such as the variance Var$[m_X]$ depend on $k_B T_{\rm MC}$ in the thermalized

TABLE I. Annotation glossary.

Symbol	Description
Variables and parameters for cells X and Y	
X, Y	Number of molecules in cells X and Y
$k_1^{\pm}, q_1^{\pm}$	Spontaneous production (+) and degradation (−) rates in cells X and Y
$k_2^{\pm}, q_2^{\pm}$	Nonlinear production (+) and degradation (−) rates in cells X and Y
h_X, h_Y	Field parameters for cells X and Y
θ_X, θ_Y	Reduced temperature parameters
m_X, m_Y	Magnetizations, scaled deviation in molecule count from n_c
γ_{xy}, γ_{yx}	Exchange rates from cell X to Y and back
g_{XY}, g_{YX}	Exchange terms in the Landau formulation
Common parameters and variables	
g	Simplified exchange parameter (set as $g_{XY} = g_{YX} = g = 1$)
n_c	Typical molecule number (system size)
H	Collective field parameter
T	Collective reduced temperature parameter
M	Collective magnetization [$M = (m_X + m_Y)/2$]
τ_d	Ramp time for driving across the transition
$I(X;Y)$	Mutual information between X and Y
$\alpha, \beta, \gamma, \delta$	Ising mean-field critical exponents

Landau model [Fig. 1(b), colored curves]. No value of $k_BT_{\rm MC}$ in the Landau simulation will truly capture the nonequilibrium Schlögl steady state [Fig. 1(b), dashed black curve]. In this paper, setting the precise value of $k_BT_{\rm MC}$ is not necessary since we focus on the mutual information between the two cells, a quantity that changes only very weakly with $k_BT_{\rm MC}$ [Fig. 1(c), colored curves].

B. Analytic Gaussian approximation

The mutual information shown in Fig. 1(c) is very well approximated by a Gaussian analytical approximation (dashed black curve). The approximation linearizes the dynamics around the deterministic fixed point, whether of the Landau model or the chemical Langevin description of the Schlögl model. This yields a multidimensional Ornstein-Uhlenbeck process [23]: $d\vec{X}_t = \mathcal{J}(\vec{X}_t - \vec{\mu})dt + \sigma d\vec{W}_t$, where $\vec{X}$ is the column vector of variables of interest, magnetizations, or molecule numbers; $\mathcal{J}$ is a negative-definite matrix; $\vec{W}$ is a vector of independent Brownian motions; and σ is a matrix. The solution is a Gaussian process in which the mutual information is completely determined by the covariance matrix. By computing the pathwise solution (see Appendix B and [23]), one finds that the stead-state covariance matrix $\mathcal{C}$ satisfies the Lyapunov equation $\mathcal{J}\mathcal{C} + \mathcal{C}\mathcal{J}^T = -\sigma\sigma^T$. This is a linear system for the coefficients of $\mathcal{C}$, so all that is left is to determine the matrices $\mathcal{J}$ and σ for the two models. For the Landau model with $0 < |H| \ll g$, we find $I_{\rm Landau} = -\frac{1}{2}\ln(1-\rho^2)$, with $\rho^2 = \frac{g^2}{(g+\overline{m}^2)^2}$ and $\overline{m} = (3H/2)^{1/3}$. Under the Gaussian approximation, the covariance matrix is proportional to $k_BT_{\rm MC}$, so the temperature cancels out when computing the correlation coefficient. Therefore, to Gaussian order, the mutual information is insensitive to the choice of $k_BT_{\rm MC}$. Since $I_{\rm Landau}$ is an even function of $\overline{m}$, the information is symmetric in H. Repeating the process for the Schlögl model, restricting ourselves to $h_X = h_Y$, we find $I_{\rm Schlögl} = -\frac{1}{2}\ln(1-\rho^2)$, with $\rho^2 = \frac{4g^2(-\overline{m}^2+\overline{m}+2)^2}{\{2g(2\overline{m}^2+\overline{m}+2)+[\overline{m}(\overline{m}+2)+4]\overline{m}^2\}^2}$. This Gaussian approximation for the Schlögl model is not even in $\overline{m}$ and is therefore asymmetric in H. As $H \to 0$, the Gaussian information diverges, indicating that the cubic terms are needed for stabilization and suggesting that the mutual information attains a maximum. For the mathematical details, see Appendix B and [23].

Setting $\theta_X = \theta_Y = T = 0$ and $h_X = h_Y$ and therefore $H = h_X + h_Y$, we calculated numerically the mutual information between X and Y at steady state for the Schlögl model and at equilibrium for the Landau case. As expected, the mutual information is maximized at the critical point, $H = 0$ [Fig. 1(d)]. The Gaussian approximation captures well the numerical simulations away from the critical point, including the asymmetry in the Schlögl case, reflecting the slightly higher information at positive H due to a higher molecule count. Interestingly, despite the typical number of molecules n_c being the same in both systems, the mutual information for the equilibrium Landau model is higher than that for the companion Schlögl model.

C. Hysteresis in the magnetization

When a system is gradually driven through a critical point, critical slowing down causes a lagged response to the driving. This phenomenon, known as the Kibble-Zurek (KZ) effect in the statistical physics literature, results in a lag that follows scaling rules governed by the critical exponents of the transition point [24–32]. Does our two-cell system exhibit KZ scaling when the collective coordinate H is driven across the transition point? While various driving protocols are possible in a biological context, when crossing the critical point, terms beyond the leading-order linear term do not asymptotically alter the critical scaling [27]. This theoretical advantage allows us to focus on a simple protocol of $H(t)$ changing linearly with time without losing biological realism—any reasonable trajectory with $H(t)$ crossing the transition point at a constant rate should scale the same.

Maintaining $T = 0$, we first let the system relax at $H = H_i = 0.1$, then varied $H(t)$ from H_i to $H_f = -0.1$ at a rate

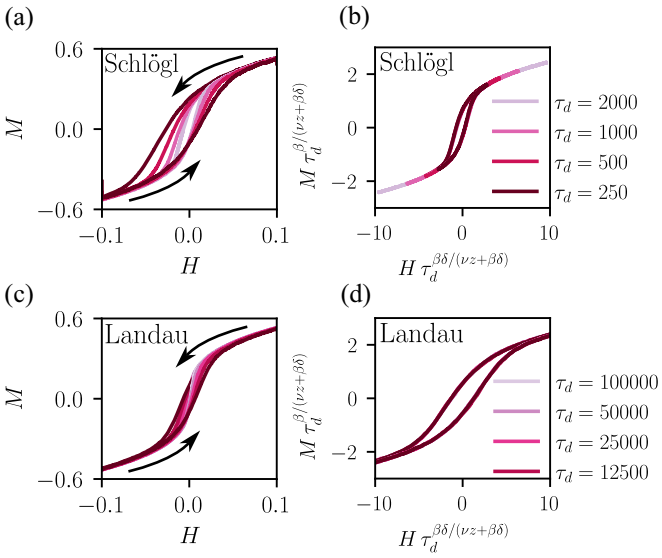

FIG. 3. Lagged response of the collective magnetization of the two-cell system, $M = (m_X + m_Y)/2$, to time-varying $H(t)$ as it is driven across the transition point at $H = 0$. The collective field $H(t)$ is ramped according to $H(t) = H_i + (H_f - H_i)/\tau_d$. The arrows indicate the direction of the ramp, starting at either $H_i = 0.1$ or -0.1. (a) Schlögl dynamics for $\tau_d = 2000, 1000, 500, 250$. To control for finite-molecule-number effects, we scale $n_c = 4\,\tau_d^{4/5}$ [11,27]. (b) The Schlögl results scaled according to the Kibble-Zurek scaling prediction. (c) The extended Landau system with $\tau_d = 100000, 50000, 25000, 12500$ and $n_c = \frac{1}{5}\,\tau_d^{4/5}$. (d) Kibble-Zurek collapse of the Landau system response. In all plots, as in the Ising mean-field universality class, $\beta = \frac{1}{2}$, $\nu z = 1$, and $\delta = 3$.

determined by τ_d, i.e., $H(t) = H_i + (H_f - H_i)/\tau_d$. Similarly, we initiated at $H_i = -0.1$ and reversed the trajectory. Importantly, to control for the damping effect of the finite-molecule number on the divergence of the correlations, the system size n_c must be scaled according to $n_c \sim \tau_d^{4/5}$ [11,27]. Consistent with KZ theory, driving across the transition induced hysteresis loops in both the Schlögl and Landau cases, with loop characteristics dependent on the ramp time τ_d and the critical exponents of the transition point. In both cases when scaled as per KZ predictions, $M\tau_d^{\beta/(\nu z+\beta\delta)} \sim H\tau_d^{\beta\delta/(\nu z+\beta\delta)}$, the Ising mean-field values for the exponents led to the collapse of the disparate hysteresis loops to a single curve (Fig. 3).

D. Flexibility in dynamics

There are many different trajectories in $\{h_X, h_Y, \theta_X, \theta_Y\}$ that have the same values for collective $\{H, T\}$. We wanted to discern whether the dynamical response of the system is sensitive only to $\{H, T\}$, even when their derivation assumed steady state. To compare the dynamical response of the system to different trajectories, we considered Eq. (3) with $H(t) = H_i + (H_f - H_i)\,t/\tau_d$ and $T = 0$, setting $H_i = 0.1$ and $H_f = -0.1$, thereby crossing the two-cell transition point $H = T = 0$. We focused on a time-varying H with a fixed $T = 0$ since it is more experimentally feasible, with h_X and h_Y corresponding to external stimuli. Since the numerical scaling collapse follows the theory, to establish the universal dynamics it suffices to show scaling in the H case. We have made all simulation code available for the interested reader to explore other scenarios. To maintain $T = 0$, we set $\theta_Y = -\frac{\theta_X}{\theta_X+1}$. Therefore, in terms of $H(t)$, the $\{h_X(t), h_Y(t)\}$ trajectories must obey $h_Y(t) = \frac{1}{1-\theta_Y/2}[H(t) - h_X(t)(1 - \frac{\theta_X/2}{\theta_X+1})]$. For the special case of $\theta_X = \theta_Y = 0$ we retrieved $h_Y(t) = H(t) - h_X(t)$, where we considered two situations: $h_Y(t) = h_X(t)$ as in Fig. 3 and $h_Y(t) = h_X(t) - 0.1$. Furthermore, we considered a third trajectory where $\theta_X(t) = 0.04 - 0.08(t/\tau_d)$ and $h_X(t) = 0.1 - 0.2(t/\tau)^2$. We chose the quadratic dependence on time to make explicit the freedom in choosing the trajectories of two of the four control parameters while maintaining the same collective dynamics. Although many other trajectories are possible, we trust that demonstrating that these three examples give identical information is enough to establish the generic flexibility in the cell-to-cell dynamics.

In contrast to the steady-state calculation (Fig. 1) in which one tracks the system over a sufficiently long time, here, to compute the information at each time step we averaged over an ensemble of independent stochastic trajectories, a significant computational effort. We found that all three driving protocols, which share the same $H(t)$ and $T(t)$, indeed have the same mutual information. As expected, the mutual information lags in response to the changing conditions (Fig. 4). As with the other results in this paper, the degeneracy between the three protocols is true for both the Schlögl dynamics and the equilibrium simulations of the companion Landau model (using Metropolis Monte Carlo).

IV. SUMMARY AND DISCUSSION

In this paper we considered a simple theoretical question with a minimal model of cell-to-cell communication: two cells that exchange a molecule and thereby share information while each cell's parameters change with time. We parameterized the stochastic dynamical system using the variables $m_X(t)$ and $m_Y(t)$, representing the activity levels or concentrations of key signaling molecules or transcription factors within cells X and Y. External stimuli $h_X(t)$ and $h_Y(t)$ correspond to external signals or environmental factors influencing each cell independently, such as hormones, nutrients, or stress signals. Damping terms $-\theta_X m_X$ and $-\theta_Y m_Y$ represent degradation processes or natural decay rates of the signaling molecules, including enzymatic breakdown or dilution due to cell growth. Nonlinear saturation terms $-\frac{m_{X,Y}^3}{3}$ account for self-regulatory feedback mechanisms, such as inhibition due to high concentrations (negative feedback loops) that prevent runaway activation. Coupling terms, $g_{XY} m_Y$, etc., describe the interaction between the two cells, such as the exchange of signaling molecules through gap junctions, synaptic connections, or paracrine signaling. Biologically, this system could represent signaling between cells, including between immune cells, coupled genetic circuits, quorum sensing, and more. Experimentally, one could apply external stimuli such as varying nutrient concentrations or chemical inducers to represent h_X and h_Y, using time-lapse fluorescence microscopy and a microfluidic device for live-cell imaging of m_X and m_Y.

We sought to discern whether cell-to-cell information sharing could be robust to varying individual cell parameters. We showed that, indeed, there are different single-cell driving protocols that lead to the same system response as long as the

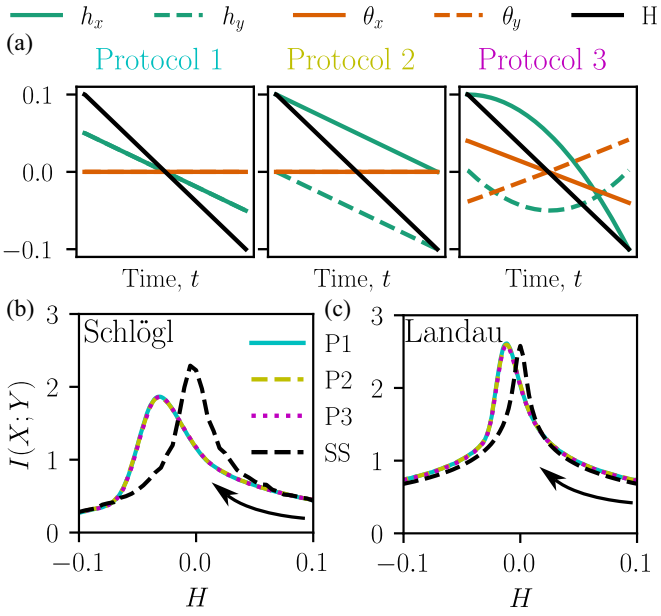

FIG. 4. Mutual information for the two-cell system with dynamically changing parameters. (a) Three different driving protocols are shown, with the same collective dynamics, $T = 0$ and $H(t) = H_i + (H_f - H_i)/\tau_d$, but different realizations of $\{h_X(t), h_Y(t), \theta_X(t), \theta_Y(t)\}$. Protocol 1: $h_X(t) = h_Y(t)$ and $\theta_X = \theta_Y = 0$; protocol 2: $h_X(t) = 0.1 + h_Y(t)$ and $\theta_X = \theta_Y = 0$; protocol 3: $\theta_X(t) = 0.04 - 0.08(t/\tau_d)$ and $h_X(t) = 0.1 - 0.2(t/\tau)^2$ (see text). (b) Mutual information calculated from the stochastic dynamics of the Schlögl model, demonstrating the same behavior of all three protocols (P1, P2, P3), with $\tau_d = 250$, showing lag and hysteresis when the transition point is crossed. Dashed lines show the steady-state mutual information from Fig. 1(d). The black arrow indicates the direction of the parameter ramp. (c) Mutual information of the companion Landau model simulated using Metropolis Monte Carlo, with $\tau_d = 6400$, showing convergence of the three protocols. Dashed lines show the equilibrium mutual information. In all simulations, $n_c = 1000$.

collective coordinates have the same dynamics. This suggests a robustness in cell-to-cell communication and a flexibility in the routes cells can take to achieve the same information-sharing outcomes. Despite the minimal nature of the model here studied, our results generalize to all models with either demographic or thermal noise that belong to the Ising mean-field universality class.

We compared the cell-to-cell stochastic dynamics of the Schlögl model with the companion equilibrium system, an extension of Landau theory that had been used in the past to describe phase transitions in minerals [16] and surface and hydration forces [17] and even more generally [18]. This is an example of KZ scaling of four-parameter nonequilibrium dynamics, here applied in the context of cell-to-cell information. Inspired by the analogy between the systems, one may consider reversing the sign of g, making the exchange molecule inhibitory, rather than excitatory, to the other cell. In the Landau formulation, this corresponds to antiferromagnetic interactions between the two subsystems. However, in the Schlögl case, one must be careful since a negative g would imply that when there are zero copies of molecule X, having nonzero Y could lead to a negative number of X molecules—a contradiction. Therefore, mechanistically, one would need to model an "interaction" where X encounters Y.

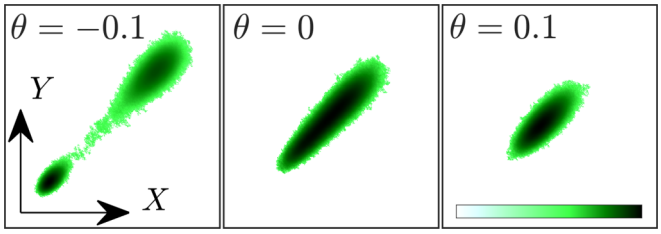

FIG. 5. Examples of the joint distribution $P(X, Y)$ shown as a heat map, calculated from Gillespie simulations of the Schlögl model [7]. The bifurcation point at $\theta = 0$ separates a bimodal from a unimodal steady state. The color map corresponds to $\log_{10} P$. In all simulations, $h_X = h_Y = 0$ and $n_c = 1000$.

The dependence of the two-cell system on its low-dimensional representation could potentially allow cells to optimize other aspects of their function without compromising information exchange, a possible mechanism for evolutionary adaptation. Indeed, such degeneracy in single-cell configurations obeying collective coordinates could extend beyond two-cell systems to entire tissues or even larger biological systems.

All code and data used for this paper are freely available from GitHub [33].

ACKNOWLEDGMENTS

Numerical simulations were paid for by A.E.'s startup funds. M.V. performed his work at the research institute AMOLF, which was funded by the Dutch Research Council (NWO) Grant No. 2019.085.

APPENDIX A: VISUALIZING THE BIFURCATION TRANSITION

To make explicit the shape of the probability distributions for the molecule counts of the two cells (X, Y), we show in Fig. 5 the effect of the bifurcation parameter θ on the two-cell collective state when $H = 0$. Note the flat-topped shape at the critical point [7].

APPENDIX B: GAUSSIAN MUTUAL INFORMATION

Linearizing a stochastic differential equation around a deterministic fixed point $\vec{\mu}$ yields an Ornstein-Uhlenbeck process [23]:

$$d\vec{X}_t = \mathcal{J}(\vec{X}_t - \vec{\mu})dt + \sigma d\vec{W}_t, \tag{B1}$$

where the matrix $\mathcal{J}$ is negative definite and $\vec{X}$ and $\vec{W}$ are column vectors. Pathwise solutions may be computed as

$$\vec{X}_t = \vec{\mu} + e^{\mathcal{J}t}(\vec{X}_0 - \vec{\mu}) + \int_0^t e^{\mathcal{J}(t-s)}\sigma d\vec{W}_s. \tag{B2}$$

Note that, for normally distributed initial conditions, this can be interpreted as a sum of normally distributed variables, so solutions are normal at all times.

The mutual information [34] between two variables V_1 and V_2 is

$$I(V_1, V_2) = \mathbb{E}\left[\ln\left(\frac{P(V_1, V_2)}{P(V_1)P(V_2)}\right)\right]. \tag{B3}$$

If V_1 and V_2 have a joint normal distribution, then this becomes

$$I(V_1, V_2) = -\frac{1}{2}\ln\left(1 - \frac{\mathrm{Cov}(V_1, V_2)^2}{\mathrm{Var}(V_1)\mathrm{Var}(V_2)}\right). \tag{B4}$$

It suffices to compute the covariance matrix of our process $\vec{X}_t$ at steady state. This can be done by subtracting the mean from Eq. (B2), right multiplying by it by its transpose, taking expectations and using the Itô isometry [23], taking $t \to \infty$, and, finally, using integration by parts. The result is that the covariance matrix $\mathcal{C}$ obeys the Lyapunov equation:

$$\mathcal{J}\mathcal{C} + \mathcal{C}\mathcal{J}^T = -\sigma\sigma^T. \tag{B5}$$

This is a linear system of equations in the coefficients of $\mathcal{C}$ that may be solved algebraically.

The matrices $\mathcal{J}$ and σ can be calculated at the level of the deterministic dynamics [Eq. (2)], so it is insensitive to the distinction between the Landau and Schlögl models. We did this in previous work [7], where, in the limit $0 < |h_X|, |h_Y| \ll g = 1$, we found

$$\overline{m}_X, \overline{m}_Y \sim \left(\frac{3(h_X + h_Y)}{2}\right)^{1/3} = \overline{m}. \tag{B6}$$

We start with the Landau dynamics. These take the form

$$\begin{aligned} dm_X &= -\Gamma\partial_{m_X} L d\tau + \sqrt{2\Gamma k_B T_{\mathrm{MC}}}\, dW_\tau^{(1)}, \\ dm_Y &= -\Gamma\partial_{m_Y} L d\tau + \sqrt{2\Gamma k_B T_{\mathrm{MC}}}\, dW_\tau^{(2)}, \end{aligned} \tag{B7}$$

where the Wiener processes used here are dimensionless (with variance τ). Linearizing the deterministic dynamics around $(m_X, m_Y) = (\overline{m}, \overline{m})$ and evaluating the noise matrix at that point, we find that

$$\mathcal{J} = -\Gamma\begin{bmatrix} g + \overline{m}^2 & -g \\ -g & g + \overline{m}^2 \end{bmatrix}, \quad \sigma = \sqrt{2\Gamma k_B T_{\mathrm{MC}}}\,\mathbb{I}_2, \tag{B8}$$

where $\mathbb{I}_2$ is the 2×2 identity matrix. Substituting Eq. (B8) into the Lyapunov equation [Eq. (B5)] and solving gives

$$\begin{aligned} \mathrm{Var}(m_X) = \mathrm{Var}(m_Y) &= \frac{k_B T_{\mathrm{MC}}(g + \overline{m}^2)}{2g\overline{m}^2 + \overline{m}^4}, \\ \mathrm{Cov}(m_X, m_Y) &= \frac{g k_B T_{\mathrm{MC}}}{2g\overline{m}^2 + \overline{m}^4}. \end{aligned} \tag{B9}$$

Therefore, the mutual information gives

$$I_{\mathrm{Landau}} = -\frac{1}{2}\ln\left(1 - \frac{g^2}{(g + \overline{m}^2)^2}\right). \tag{B10}$$

Because the covariance matrix was proportional to T_{MC} under this approximation, this Monte Carlo completely cancels out from the mutual information at the Gaussian limit. Additionally, note that this expression is even in $\overline{m}$ and therefore in H.

Now we turn to the case of the Schlögl model, which has demographic noise. The dynamics under the chemical Langevin approximation [20] can be written as

$$\begin{aligned} dx_t &= \left(k_1^+ - k_1^- x_t + k_2^+ x_t^2 - k_2^- x_t^3 + \gamma_{YX} y_t - \gamma_{XY} x_t\right)dt \\ &\quad + \sqrt{k_1^+ + k_1^- x_t + k_2^+ x_t^2 + k_2^- x_t^3}\, dW_t^{(1)} \\ &\quad - \sqrt{\gamma_{XY} x_t}\, dW_t^{(3)} + \sqrt{\gamma_{YX} y_t}\, dW_t^{(4)}, \\ dy_t &= \left(q_1^+ - q_1^- y_t + q_2^+ y_t^2 - q_2^- y_t^3 - \gamma_{YX} y_t + \gamma_{XY} x_t\right)dt \\ &\quad + \sqrt{q_1^+ + q_1^- y_t + q_2^+ y_t^2 + q_2^- y_t^3}\, dW_t^{(2)} \\ &\quad + \sqrt{\gamma_{XY} x_t}\, dW_t^{(3)} - \sqrt{\gamma_{YX} y_t}\, dW_t^{(4)}. \end{aligned} \tag{B11}$$

In previous work, we inverted the relations between the Landau parameters and the chemical reaction rates [7]. If we have $n_c \gg 1$ and $\theta_X = \theta_Y = 0$, the inverse mapping becomes

$$\begin{aligned} &q_1^- = k_1^-, \quad \gamma_{XY} = \gamma_{YX} = g k_1^-, \quad k_1^+ = n_c k_1^-(h_X + 1/3), \\ &q_1^+ = n_c k_1^-(h_Y + 1/3), \quad k_2^- = q_2^- = k_1^-/\left(3n_c^2\right), \\ &k_2^+ = q_2^+ = k_1^-/n_c. \end{aligned} \tag{B12}$$

We define the mean reactive/nonexchange propensity for X as

$$\begin{aligned} \overline{R}_X &= k_1^+ + k_1^-\overline{x} + k_2^+\overline{x}^2 + k_2^-\overline{x}^3 \\ &= n_c k_1^-\left[h_X + 1/3 + (\overline{m} + 1) + (\overline{m} + 1)^2 + \frac{(\overline{m} + 1)^3}{3}\right] \\ &= n_c k_1^-\left[h_X + 8/3 + 4\overline{m} + 2\overline{m}^2 + \frac{\overline{m}^3}{3}\right]. \end{aligned} \tag{B13}$$

Analogously, for Y, we have

$$\overline{R}_Y = n_c k_1^-\left[h_Y + 8/3 + 4\overline{m} + 2\overline{m}^2 + \frac{\overline{m}^3}{3}\right]. \tag{B14}$$

Finally, we define the mean diffusive propensity as

$$\overline{D} = \gamma_{XY}\overline{x} = g k_1^- n_c(\overline{m} + 1). \tag{B15}$$

The noise matrix in the linearization is the matrix evaluated at $(x, y) = (n_c(\overline{m} + 1), n_c(\overline{m} + 1))$. We find that

$$\sigma = \begin{bmatrix} \sqrt{\overline{R}_X} & 0 & -\sqrt{\overline{D}} & \sqrt{\overline{D}} \\ 0 & \sqrt{\overline{R}_Y} & \sqrt{\overline{D}} & -\sqrt{\overline{D}} \end{bmatrix}. \tag{B16}$$

Evaluating the derivative of the deterministic part at the fixed point gives

$$\mathcal{J} = -k_1^-\begin{bmatrix} g + \overline{m}^2 & -g \\ -g & g + \overline{m}^2 \end{bmatrix}, \tag{B17}$$

which is proportional to the result from the Landau case. It is readily apparent that σ is not even in $\overline{m}$, so we expect asymmetry in H with demographic noise. The case with $h_X = h_Y$ allows some simplification:

$$\begin{aligned} I_{\mathrm{Schlögl}} &= -\frac{1}{2}\ln(1 - \rho^2) \\ \rho^2 &= \frac{4g^2(-\overline{m}^2 + \overline{m} + 2)^2}{\{2g(2\overline{m}^2 + \overline{m} + 2) + [\overline{m}(\overline{m} + 2) + 4]\overline{m}^2\}^2}. \end{aligned} \tag{B18}$$

In the general case where $h_X \neq h_Y$, the expression is messy and is studied numerically.

[1] V. Ngampruetikorn, D. J. Schwab, and G. J. Stephens, Energy consumption and cooperation for optimal sensing, Nat. Commun. **11**, 975 (2020).

[2] T. R. Sokolowski and G. Tkačik, Optimizing information flow in small genetic networks. IV. Spatial coupling, Phys. Rev. E **91**, 062710 (2015).

[3] G. Tkačik and T. Gregor, The many bits of positional information, Development **148**, dev176065 (2021).

[4] S. J. Bryant and B. B. Machta, Physical constraints in intracellular signaling: The cost of sending a bit, Phys. Rev. Lett. **131**, 068401 (2023).

[5] A. J. Tjalma, V. Galstyan, J. Goedhart, L. Slim, N. B. Becker, and P. R. ten Wolde, Trade-offs between cost and information in cellular prediction, Proc. Natl. Acad. Sci. USA **120**, e2303078120 (2023).

[6] A. Erez, T. A. Byrd, R. M. Vogel, G. Altan-Bonnet, and A. Mugler, Universality of biochemical feedback and its application to immune cells, Phys. Rev. E **99**, 022422 (2019).

[7] A. Erez, T. A. Byrd, M. Vennettilli, and A. Mugler, Cell-to-cell information at a feedback-induced bifurcation point, Phys. Rev. Lett. **125**, 048103 (2020).

[8] R. M. Vogel, A. Erez, and G. Altan-Bonnet, Dichotomy of cellular inhibition by small-molecule inhibitors revealed by single-cell analysis, Nat. Commun. **7**, 12428 (2016).

[9] A. Erez, R. Vogel, A. Mugler, A. Belmonte, and G. Altan-Bonnet, Modeling of cytometry data in logarithmic space: When is a bimodal distribution not bimodal? Cytometry, Part A **93**, 611 (2018).

[10] G. Altan-Bonnet and R. N. Germain, Modeling T cell antigen discrimination based on feedback control of digital ERK responses, PLoS Biol. **3**, e356 (2005).

[11] T. A. Byrd, A. Erez, R. M. Vogel, C. Peterson, M. Vennettilli, G. Altan-Bonnet, and A. Mugler, Critical slowing down in biochemical networks with feedback, Phys. Rev. E **100**, 022415 (2019).

[12] F. Schlögl, Chemical reaction models for non-equilibrium phase transitions, Z. Phys. **253**, 147 (1972).

[13] P. Grassberger, On phase transitions in Schlögl's second model, Z. Phys. B **47**, 365 (1982).

[14] I. Bose and S. Ghosh, Bifurcation and criticality, J. Stat. Mech. (2019) 043403.

[15] M. Vennettilli, A. Erez, and A. Mugler, Multicellular sensing at a feedback-induced critical point, Phys. Rev. E **102**, 052411 (2020).

[16] E. K. H. Salje, Application of Landau theory for the analysis of phase transitions in minerals, Phys. Rep. **215**, 49 (1992).

[17] A. A. Kornyshev, D. A. Kossakowski, and S. Leikin, Surface phase transitions and hydration forces, J. Chem. Phys. **97**, 6809 (1992).

[18] A. A. Kornyshev, D. A. Kossakowski, and S. Leikin, Landau theory of a system with two bilinearly coupled order parameter sin external field: Exact mean field solution, critical properties and isothermal susceptibility, Z. Naturforsch. A **50**, 789 (1995).

[19] D. T. Gillespie, A general method for numerically simulating the stochastic time evolution of coupled chemical reactions, J. Comput. Phys. **22**, 403 (1976).

[20] D. T. Gillespie, The chemical Langevin equation, J. Chem. Phys. **113**, 297 (2000).

[21] P. C. Hohenberg and B. I. Halperin, Theory of dynamic critical phenomena, Rev. Mod. Phys. **49**, 435 (1977).

[22] N. Goldenfeld, *Lectures on Phase Transitions and the Renormalization Group*, Frontiers in Physics (Addison-Wesley, Reading, MA, 1992), Vol. 85.

[23] F. C. Klebaner, *Introduction to Stochastic Calculus with Applications* (World Scientific, Singapore, 2012).

[24] T. W. B. Kibble, Topology of cosmic domains and strings, J. Phys. A **9**, 1387 (1976).

[25] W. H. Zurek, Cosmological experiments in superfluid helium? Nature (London) **317**, 505 (1985).

[26] G. Biroli, L. F. Cugliandolo, and A. Sicilia, Kibble-Zurek mechanism and infinitely slow annealing through critical points, Phys. Rev. E **81**, 050101(R) (2010).

[27] A. Chandran, A. Erez, S. S. Gubser, and S. L. Sondhi, Kibble-Zurek problem: Universality and the scaling limit, Phys. Rev. B **86**, 064304 (2012).

[28] S. Deffner, Kibble-Zurek scaling of the irreversible entropy production, Phys. Rev. E **96**, 052125 (2017).

[29] H. Fujita, M. Nishida, M. Nozaki, and Y. Sugimoto, Dynamics of logarithmic negativity and mutual information in smooth quenches, Prog. Theor. Exp. Phys. **2020**, 073B02 (2020).

[30] D. Proverbio, A. N. Montanari, A. Skupin, and J. Gonçalves, Buffering variability in cell regulation motifs close to criticality, Phys. Rev. E **106**, L032402 (2022).

[31] F. Tarantelli and E. Vicari, Out-of-equilibrium dynamics arising from slow round-trip variations of Hamiltonian parameters across quantum and classical critical points, Phys. Rev. B **105**, 235124 (2022).

[32] A. Berger, M. G. Harari, A. Gross, and A. Erez, Diversity loss in microbial ecosystems undergoing gradual environmental changes, Cell Reports Sustainability **1**, 100242 (2024).

[33] https://github.com/AmirErez/TwocellInformationPy.

[34] C. E. Shannon, A mathematical theory of communication, Bell Syst. Tech. J. **27**, 379 (1948).